JOURNAL OF APPLIED POLYMER SCIENCE VOL. 16, PP. 361-380 (1972)

# Time–Temperature Superposition of Large-Strain Shear Properties of the Ethylene–Propylene Copolymer System

S. BAHADUR* AND K. C. LUDEMA, *University of Michigan, College of Engineering, Ann Arbor, Michigan 48104*

## Synopsis

The principle of time temperature superposition for some mechanical properties of polymers is well known, particularly where strains are on the order of 1% or less. For large strains the simple data transformation techniques are not useful, probably because of morphological changes in the polymer. Morphological changes have the effect of changing the mechanical properties, thus necessitating a shift on the verticle axis as well as horizontal axis where mechanical properties are plotted on the ordinate and strain rate, e.g., is plotted on the abscissa. By the Rouse and Zimm theories of flexible chain polymer molecules a relationship is shown between a verticle shift and a horizontal shift, thereby making it unnecessary to determine the exact nature of morphological changes in the polymer when strained. Six polymers were strained to the fracture point and the shear modulus and fracture strength data were used to demonstrate the technique of simultaneous verticle and horizontal transformation of data.

## INTRODUCTION

The mechanical properties of polymers are highly strain-rate and temperature dependent. The effects of temperature and strain rate are interdependent, making feasible a time–temperature transformation of such linear viscoelastic properties as stress relaxation modulus, creep compliance, and dynamic moduli. The interdependence is often expressed as a "shift factor," $a_T$, which implies the horizontal shift needed for the data points (representing the mechanical properties plotted on the ordinate against strain rate on the abscissa) at a temperature to correspond to the data points at some other temperature. Two equations, originally derived empirically but later verified theoretically, express the extent of horizontal shift with change in temperature. In the temperature range $T_g$ to ($T_g$ + 100°C), the WLF equation[1]

$$\log a_T = \frac{-8.86\ (T - T_s)}{101.6 + T - T_s}$$

* Present address: College of Engineering, State University of Iowa, Ames, Iowa 50010.

is used, where $T_s = (T_g + 50°C)$ and $T_g$ is the glass transition temperature. Outside this temperature range, the shift factor is calculated from an equation of the Arrhenius form[1]

$$\log a_T = \frac{H_a}{R}\left(\frac{1}{T} - \frac{1}{T_0}\right)$$

where $H_a$ is the activation energy for the particular transition of interest, $R$ is the universal gas constant, and $T_0$ is the temperature selected as reference. In both of these equations, $T$ is the temperature for which the data is being considered. The Arrhenius equation is not used in the glass transition region because in this domain the activation energy is a strong function of temperature. The WLF equation is used for amorphous and low-crystallinity polymers, while the Arrhenius equation is applied to moderately crystalline and highly crystalline polymers. The principle of superposition (transformation) requires that all the relaxation times have the same temperature dependence. This is satisfied strictly by the amorphous phase of polymer only. The extension of this principle to other phases of polymer is therefore made with certain reservations. Likewise, the extension of this principle to properties involving large strains must be made with great caution due to strain-induced crystallization in the polymer.

However, there is evidence that polymer properties involving large strains may also be transformed. For example, Halpin and Bueche[2] demonstrated the applicability of time–temperature superposition by successfully obtaining a master curve from the fracture stress data of styrene–butadiene and ethylene–propylene copolymers in rubbery phases. Smith[3] transformed the fracture stress data of unfilled vulcanizates of silicone, butyl rubber, and Viton B (hydrofluorocarbon elastomer) in the rubber phases using the WLF equation. Brettschneider[4] was successful in transforming the tensile properties of Thiokol propellant type P (ammonium perchlorate oxidizer dispersed in elastomeric binder) in the rubbery phase. Holt[5] was also able to construct a master curve from compressive stress data corresponding to 2% strain of poly(methyl methacrylate).

On the other hand, the superposition procedure has been found inapplicable for the following cases. Holt[5] found it impossible to transform the compressive stress data for 8% to 10% strain in poly(methyl methacrylate). Smith[3] found that he could not transform the fracture strength values of natural rubber below 90°C. The failure in these cases is thought to be due to strain-induced crystallization. Lohr[6] attempted to transform the yield strength for a number of crystalline and amorphous polymers in the glassy region without success. He shifted the curves empirically but found that the shift factors could not be expressed by an equation of the Arrhenius form.

## DEVELOPMENT OF TIME-TEMPERATURE SUPERPOSITION PROCEDURE

The WLF equation and the Arrhenius equation seem to be applicable as long as the molecule behaves as a flexible chain. When the rigidity of the molecular backbone reaches some limit either because of a great number of entanglements (as in glassy polymers) or because of a large number of crosslinks, the simple transforms are no longer applicable. A new superposition procedure is found to apply to such cases. The procedure suggested here has its basis in the theoretical work of Ferry[1] and Tobolsky,[7] who used the Rouse and Zimm theories of flexible-chain polymer molecules. It has, however, been extended to account for the entanglement couplings, which are conceived to be in the nature of transient crosslinks formed by the association of loci with strong attractive forces. Since the formation of such linkages will depend on local conditions, the polymer molecule is likely to encounter varying resistance at different locations. Taking these factors into account, Beuche[8] has made some calculations for mechanical compliance of high molecular entanglement network. Marvin[9] modified the theory and called it a ladder network. The complex shear modulus expression for Marvin's ladder model is

$$G' + iG'' = \frac{5\rho RT}{6m} \cdot (p_R)^{1/2} \times \frac{\tanh (p_R)^{1/2} + \left(\frac{M}{2m}\right)^{1.2} \cdot \tanh\left(\frac{M}{2m} - 1\right)\left[p_R\left(\frac{M}{2m}\right)^{2.4}\right]^{1/}}{1 + \left(\frac{M}{2m}\right)^{1.2} \cdot \tanh p_R \cdot \tanh\left(\frac{M}{2m} - 1\right)\left[p_R\left(\frac{M}{2m}\right)^{2.4}\right]^{1/2}}$$

where

$$p_R = i\omega\left(\frac{3a^2\xi_0}{50kT}\right)\left(\frac{m}{M_0}\right)^2$$

and $M$ = average molecular weight of polymer, $m$ = average molecular weight between entanglement coupling points, $M_0$ = molecular weight of a monomer unit, $\rho$ = density, $R$ = universal gas constant, $T$ = temperature, $k$ = Boltzmann's constant, $a$ = monomer length, $\xi_0$ = monomeric friction coefficient, and $\omega$ = frequency.

It is not possible to solve this complex expression independently for $G'$ and $G''$. A numerical solution for this equation by Lovell for several $(M/2m)$ and $p_R$ values is tabulated in ref. 1. It is found that $G'$ and $G''$ are the same for all values of $(M/2m)$ when $p_R/i \geqslant 25$. A rough calculation showed that for all high polymers under the practical test conditions, $p_R/i$ is much greater than 25.

An approximate evaluation of the above equation gives the magnitude and frequency location for a maximum in loss modulus, $G''$, by the following equation[1]:

$$G''_{\max} = 0.32\rho(RT/m)$$

$$(\omega)G''_{\max} = (95kT/a^2\xi_0 z^2)(m/M)^{1/2}$$

where $z$ is the degree of polymerization. Thus, for temperatures $T_0$ and $T$,

$$\frac{G''_{\max}}{G''_{0\max}} \alpha \frac{m_0}{m}$$

and

$$\frac{(\omega)G''_{\max}}{(\omega)G''_{0\max}} \alpha \left(\frac{m}{m_0}\right)^{1/2}$$

where $G''_{\max}$ and $G''_{0\max}$ are the maximum loss moduli corresponding to temperatures $T$ and $T_0$, respectively, and $(\omega)G''_{\max}$ and $(\omega)G''_{0\max}$ are the corresponding frequencies.

For the sake of analysis, it may be assumed without sufficient error that the transient crosslinks are uniformly distributed. Thus, the larger the number of transient crosslinks or network strands per unit volume, $n$, the smaller is $m$, so that $n \alpha 1/m$.

If with a change in temperature from $T_0$ to $T$, the network density changes by a factor $f$, we have $f = n/n_0 \alpha m_0/m$. Thus,

$$\frac{G''_{\max}}{G''_{0\max}} \alpha f$$

and

$$\frac{(\omega)G''_{\max}}{(\omega)G''_{0\max}} \alpha \frac{1}{f^{1/2}}.$$

The important point of the above development is that viscoelastic transforms for the case of molecular entanglement involve both vertical as well as horizontal shifts. The equations show that the maximum $G''$ ($G'$, or $G$ for nonperiodic loading) at a temperature $T$ would be $f$ times higher than its value at a higher temperature $T_0$ due to an increase in entanglement couplings with temperature. At the same time, the frequency or strain rate for maximum modulus at temperature $T$ would be lower by a factor $f^{1/2}$. Since the shear strength of polymer also increases with an increase in entanglement couplings, the conclusions for shear modulus may be considered true for shear strength as well. In principle, the above should also be true for other viscoelastic properties. However, the value of $f$ would be found different for different properties with the same temperature change.

The superposition procedure involving both vertical and horizontal shifts may now be set down. From the several curves of mechanical property plotted against strain rate, a reference curve may be selected.

All of the other curves for different temperatures may then be shifted horizontally and vertically so as to superimpose on the reference curve as best as possible. The horizontal shift on logarithmic scale may be designated by log $a_T$, and the vertical shift, by log $(1/f)$. Since the effect of increase in entanglement couplings is to reduce the shift by a factor $f^{1/2}$, the shift, in the absence of the effect of entanglement couplings, would be $a_T(f^{1/2})$. This is the shift expected if the polymer molecule were to behave as a flexible chain. Since the time–temperature interdependence in the glassy as well as in the crystalline rubbery states is governed by the Arrhenius equation, the plot of log $(a_T f^{1/2})$ versus $(1/T - 1/T_0)$ should give a straight line (where $T_0$ is the reference temperature and $T$ is any other test temperature). The slope of a straight line drawn through the plotted points provides $H_a/R$, so that the activation energy $H_a$ can be calculated. The data points corresponding to the different test temperatures shifted vertically by log $(1/f)$ and horizontally by log $(a_T f^{1/2})$, as read from this straight line, give rise to a master curve at the reference temperature. It must be realized that this is a trial-and-error procedure and is very tedious. One does not know exactly how much to shift the data curves horizontally and vertically until considerable experience is gained. After some practice, one converges readily and obtains a straight line on the plot of log $(a_T f^{1/2})$ versus $(1/T - 1/T_0)$. The above method will be demonstrated with the data gathered in the manner described below.

## EXPERIMENTAL

It was decided to measure two properties connected with distinctly different magnitudes of strain. Furthermore, it was decided to avoid crossing the boundaries between two basic types of deformation, namely, shear and bulk dilation. Thus, a shear test to failure was selected. A continuous plot of force versus deflection of the specimen was obtained from which the values of shear modulus and shear strength were calculated. The tests were performed over a large range of strain rates and temperatures. The test specimen selected was the tensile loaded double-shear configuration (after Zapel[10]), shown in Figure 1. This configuration was chosen because of the extensive amount of photoelastic studies of shear stress distribution made with this configuration. The dimensions shown in Figure 1 turn out to be critical when using combinations of high strain rate and low temperature because of the prominence of brittle fracture under these conditions. All of the specimens were cut from $\frac{1}{8}$-in.-thick sheet, the slots were cut by a band saw, and the holes were drilled with the use of a jig.

Straining of the specimen was effected by separation of pins inserted into the $\frac{1}{4}$-in.-diameter holes in the specimen. The separation rate of the pins could be varied over a range of 1500 to 1. Shear strain rates were determined by a number of methods and could be related to the pin separation rates. The effective strain rate range for the shear modulus test was from 0.1 to 22.0 in./in./sec, and for the shear strength test the range was from

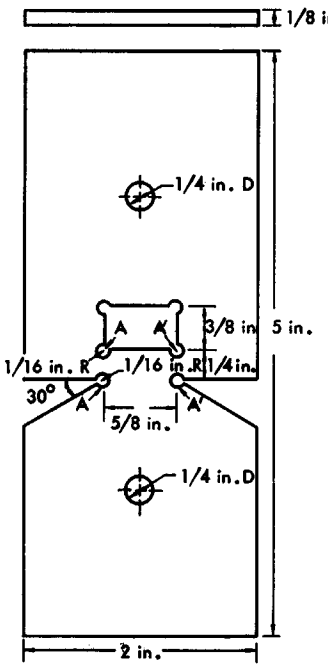


Fig. 1. Double-shear specimen configuration.

0.525 to 888.0 in./in./sec. From one trace of force versus pin separation rate for each specimen, the shear modulus and the shear strength were determined. The disparity between the strain rate range for the shear strength and the strain rate range for the shear modulus data arises from the changing strain pattern in the material as pin separation increased. At

TABLE I
Identification of Polymers Tested

| | % Ethylene | % Propylene | Density[a] | % Crystallinity[a] | $T'_g$[a] |
|---|---|---|---|---|---|
| Polymers | | | | | |
| Linear (high-density) polyethylene | | | ~0.96 | >90 | −120°C |
| Branched (low-density)polyethylene | | | ~0.92 | ~55 | −120°C |
| Atactic polypropylene | | | — | ~10 | −20°C |
| Copolymers | | | | | |
| Vistalon 3708 | 75 | 22[b] | | 1–2 | −50°C |
| Vistalon 6505 | 60 | 31[b] | | — | −45°C |
| Vistalon 404 | 40 | 60 | | — | −55°C |

[a] Values are as reported in the literature for the class of material and so are merely approximate.

[b] Balance is unsaturated material.

low strains, the shear band was some five times as wide as the shear band at the point of failure of the specimen.

The temperature range of the test extended from −155°C to +24°C, the actual range depending upon the individual polymer. The temperature of the specimens was known to within a 2°C accuracy.

Six materials were tested. Some of their properties are shown in Table I. The high-density and low-density polyethylenes were of commercial grade. The polypropylene was supplied from bulk stock without the addition of plasticizers. The ethylene–propylene copolymers were supplied by Enjay Polymer Laboratories in the form of the basic stock used in their series of products with the trade name Vistalon. The commercial designations have been used for Vistalon throughout, even though the materials tested contained no SRF black, calcium stearate, DiCup 40C, sulfur, etc. The only consideration exercised in selecting the polymers was to cover a range of glassiness and crystallinity.

## TRANSFORMATION OF EXPERIMENTAL DATA

The data obtained from each test are of a form shown in Figure 2. Because of some difficulty in measuring the initial slope of the force–extension curve, it was approximated as the slope of curve A shown in Figure 2. The shear strength data were taken from the point of failure shown as point B in the same figure.

Some scatter was observed in the data. Burchett,[11] Hsiao and Sauer,[12] Olear and Erdogan,[13] and others have also reported similar scatter in their measured data. The scatter in data seems typical and is probably unavoidable because of the anisotropy, nonhomogeneity, and internal flaws

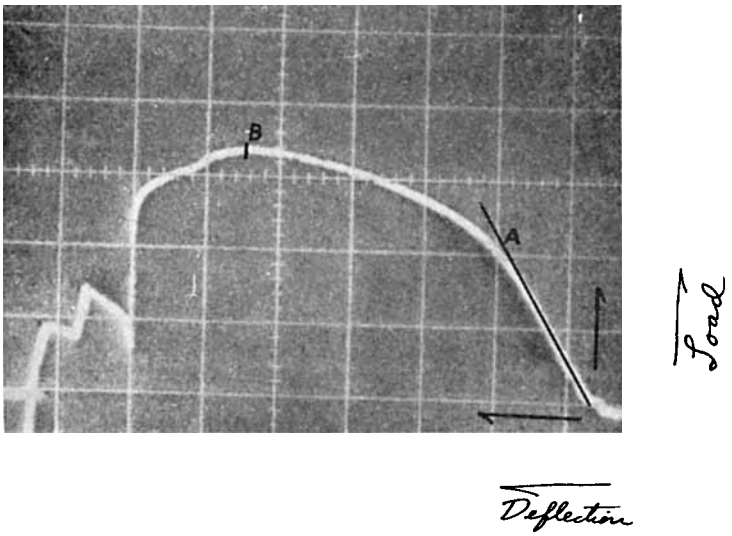


Fig. 2. Oscilloscope record of force vs. extension from shear test.

inherent in even the most carefully prepared specimens. The data reported in this paper contain many points that were checked by repeating the test.

Figures 3 through 8 show the shear strength versus logarithm of the shear strain rate at various temperatures for the six materials tested. Figures 9

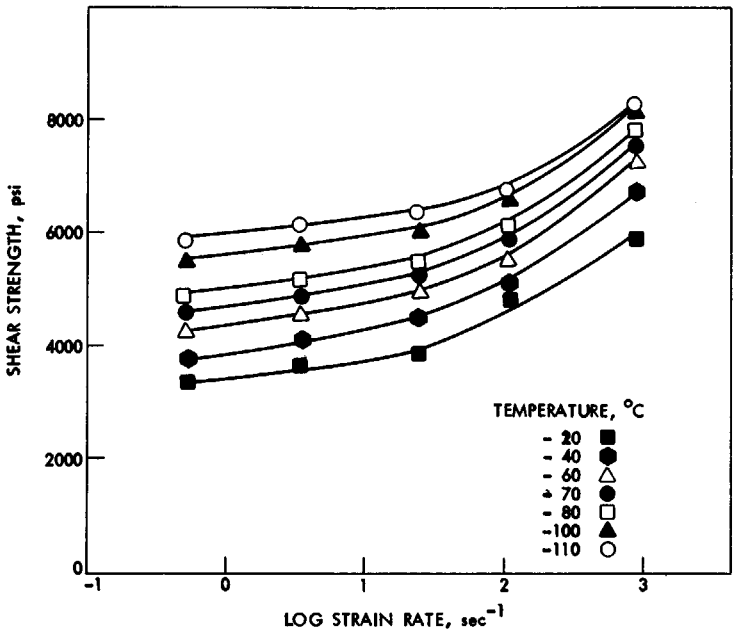


Fig. 3. Shear strength vs. strain rate at various temperatures for linear polyethylene.

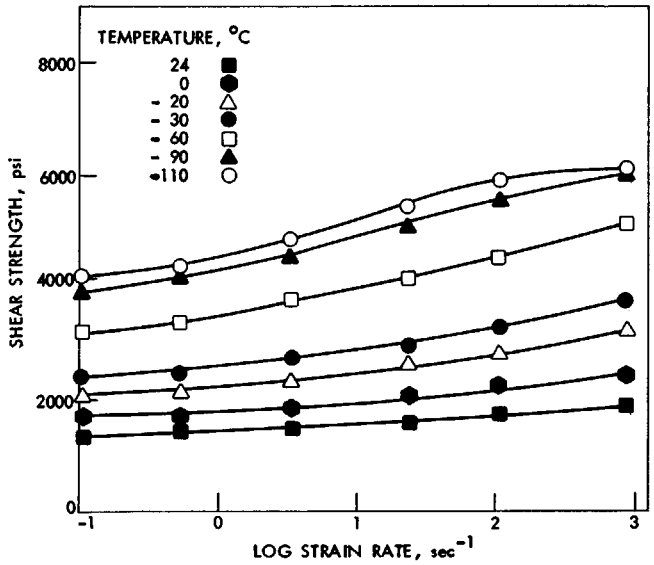


Fig. 4. Shear strength vs. strain rate at various temperatures for branched polyethylene.

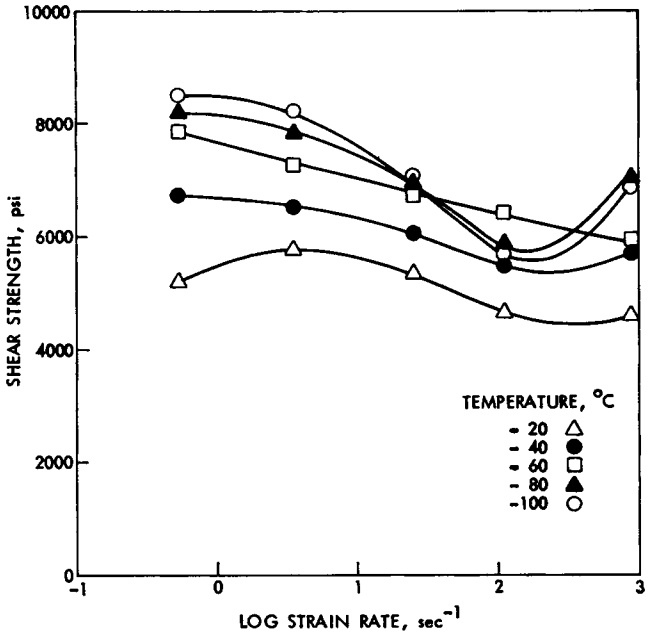


Fig. 5. Shear strength vs. strain rate at various temperatures for atactic polypropylene.

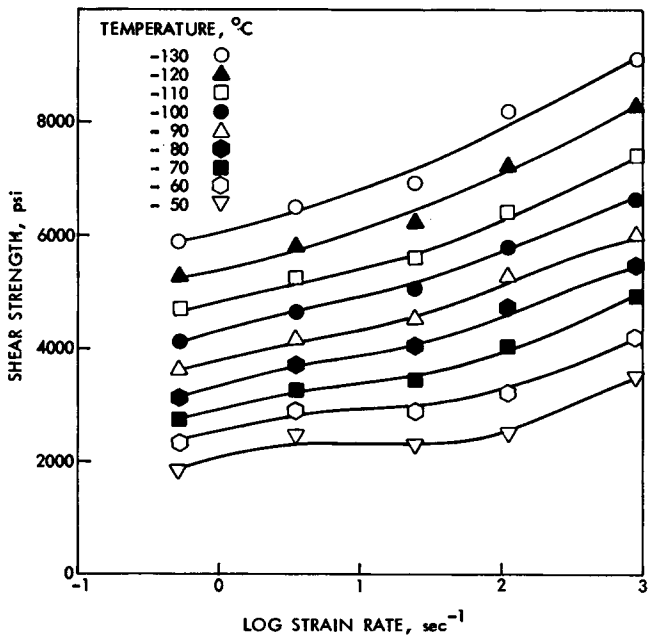


Fig. 6. Shear strength vs. strain rate at various temperatures for Vistalon 3708.

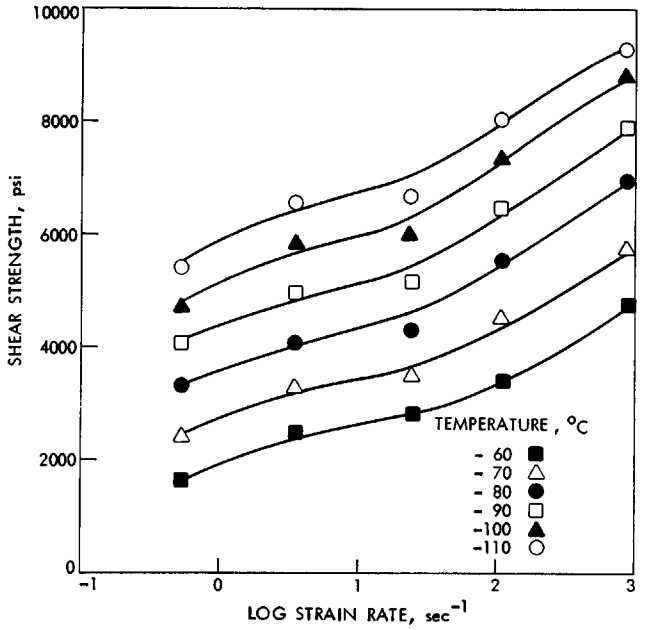


Fig. 7. Shear strength vs. strain rate at various temperatures for Vistalon 6505.

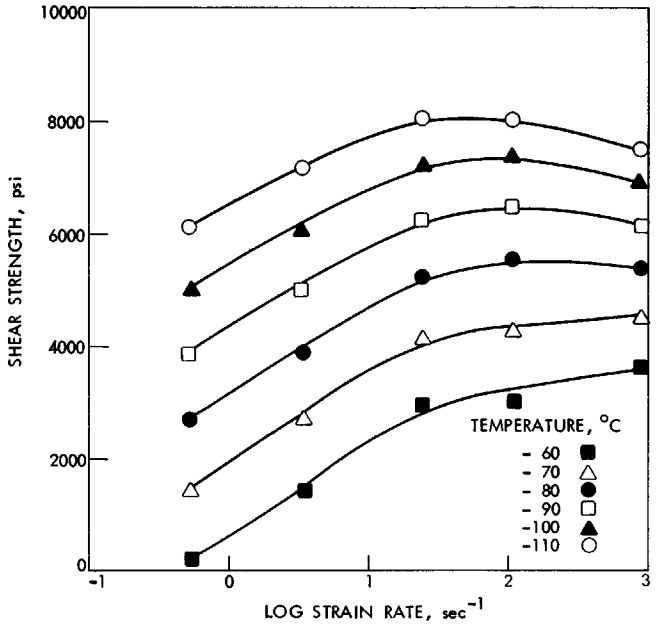


Fig. 8. Shear strength vs. strain rate at various temperatures for Vistalon 404.

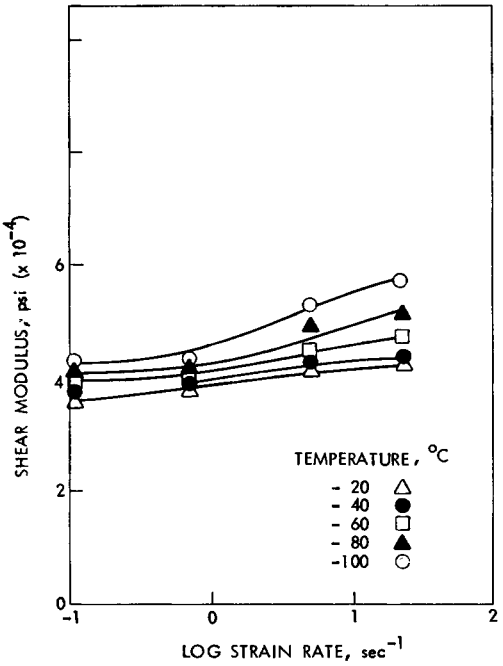


Fig. 9. Shear modulus vs. strain rate for linear polyethylene.

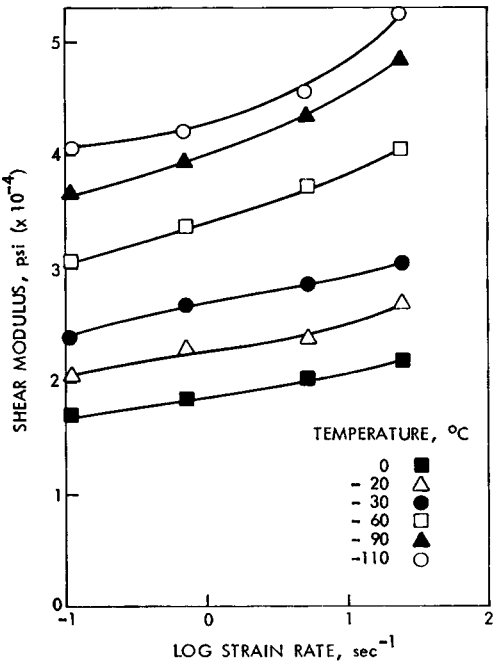


Fig. 10. Shear modulus vs. strain rate for branched polyethylene.

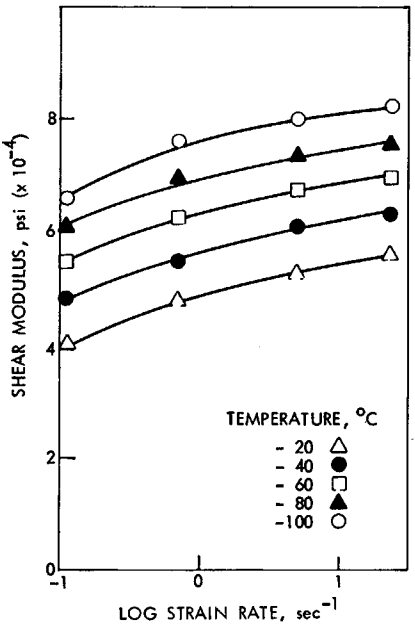


Fig. 11. Shear modulus vs. strain rate for atactic polypropylene.

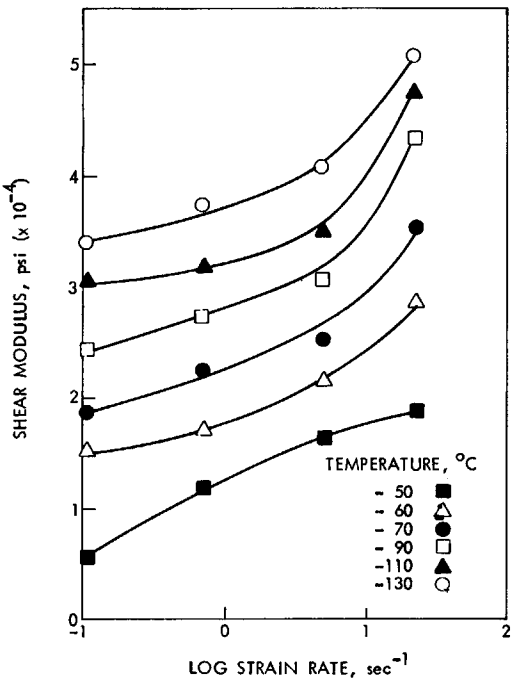


Fig. 12. Shear modulus vs. strain rate at various temperatures for Vistalon 3708.

through 14 show the shear modulus versus logarithm of the strain rate at various temperatures for the same six materials. All of these plots show that the shear strength and shear modulus of polymers increase with increasing strain rate and with decreasing temperature. One exception is the branched polyethylene, which is nearly strain-rate insensitive except at very low temperatures. This is an observation in agreement with Ely.[14]

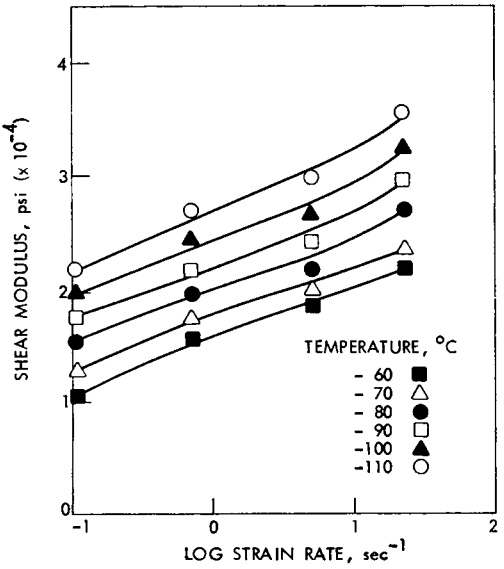


Fig. 13. Shear modulus vs. strain rate for Vistalon 6505.

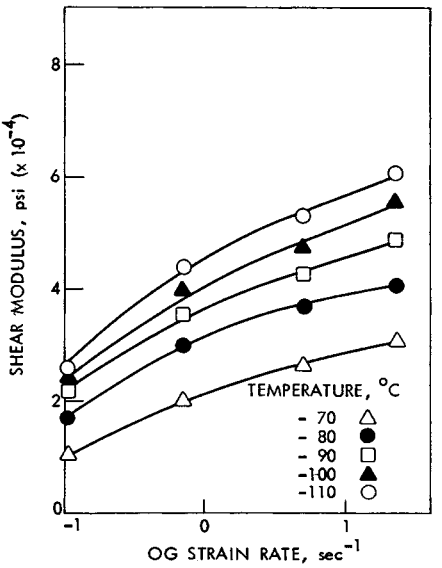


Fig. 14. Shear modulus vs. strain rate for Vistalon 404.

Another exception is the shear strength of the polypropylene, which appears to decrease as strain rate increases to a minimum value at 200 in./in./sec strain rate, after which it rises, particularly at −80°C and −100°C. The latter reversal in behavior may indicate a molecular transition.

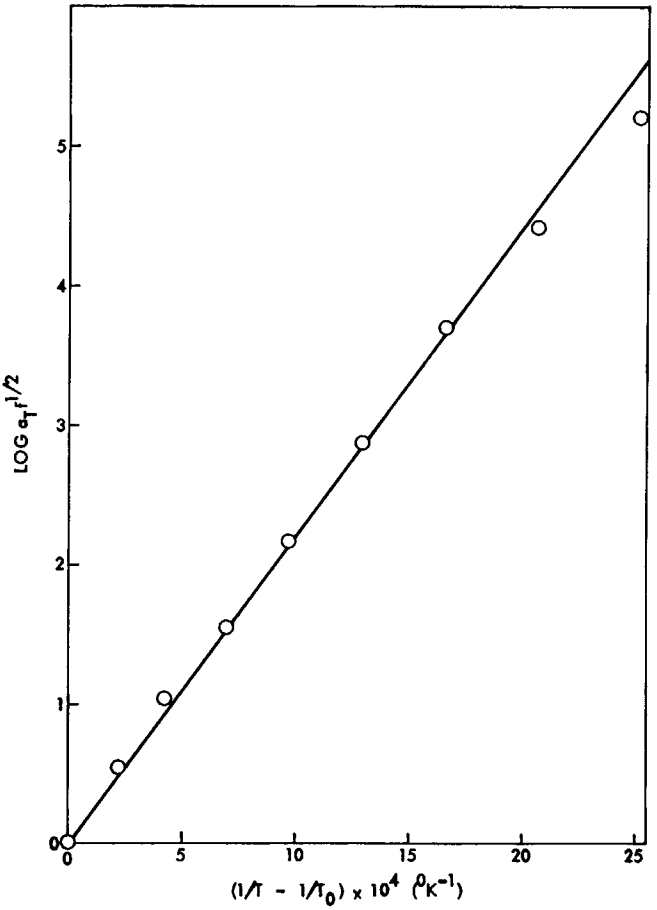


Fig. 15. Arrhenius plot for shear strength data of Vistalon 3708.

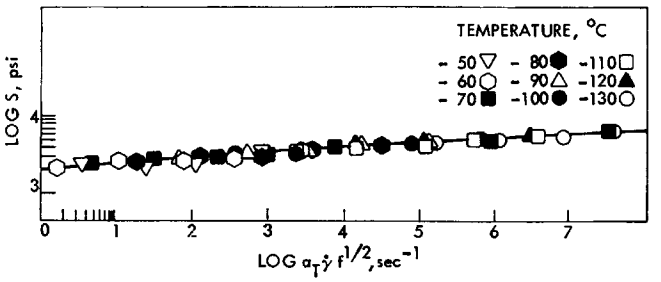


Fig. 16. Shear strength vs. strain rate master curve at −50°C for Vistalon 3708.

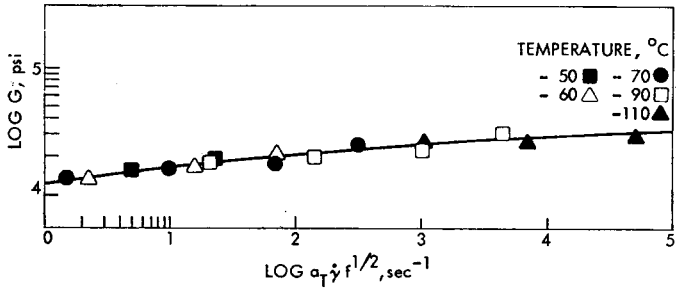


Fig. 17. Shear modulus vs. strain rate master curve at −50°C for Vistalon 3708.

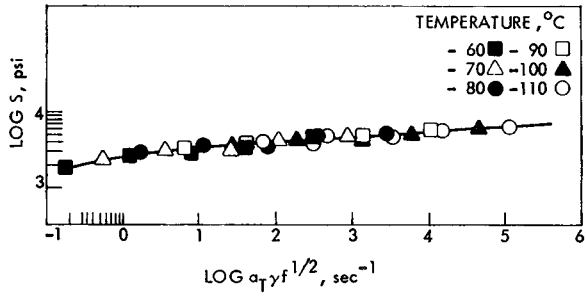


Fig. 18. Shear strength vs. strain rate master curve at −70°C for Vistalon 6505.

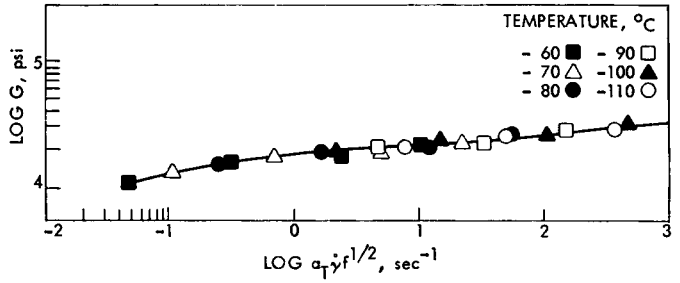


Fig. 19. Shear modulus vs. strain rate master curve at −70°C for Vistalon 6505.

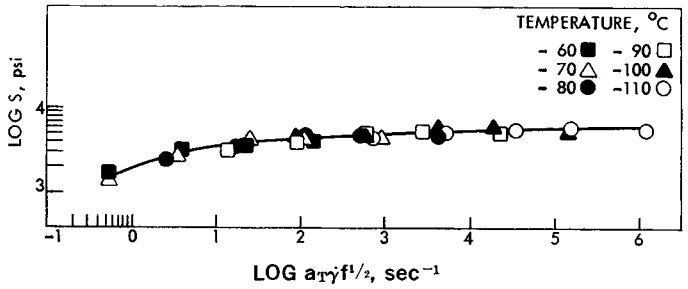


Fig. 20. Shear strength vs. strain rate master curve at −70°C for Vistalon 404.

It may also be observed that the Vistalons behave in accord with their major constituent. The Vistalons 3708 and 6504, which have high ethylene contents, behave similar to the low-crystallinity polyethylene. On the other hand, Vistalon 404 behaves more like the polypropylene.

The transformation of the shear data was to some extent guided by the knowledge of the glass transition temperature and the likely crystallinity of

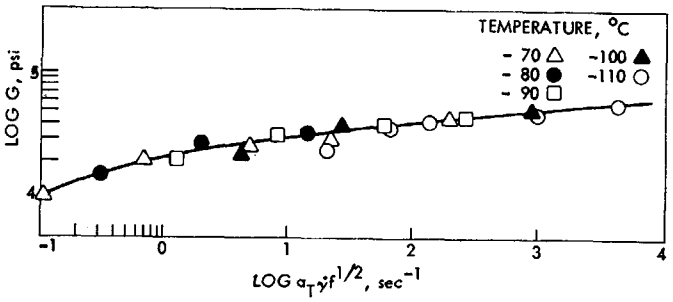


Fig. 21. Shear modulus vs. strain rate master curve at −70°C for Vistalon 404.

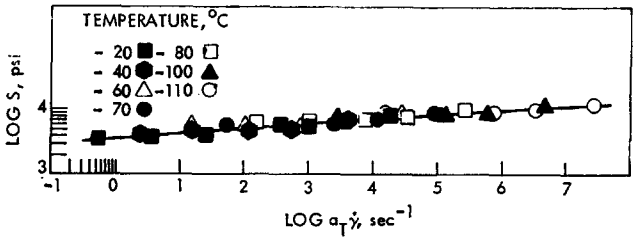


Fig. 22. Shear strength vs. strain rate master curve at −20°C for linear polyethylene.

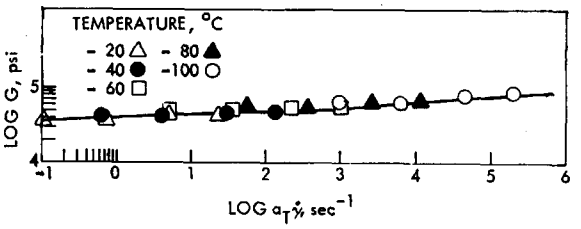


Fig. 23. Shear modulus vs. strain rate master curve at −20°C for linear polyethylene.

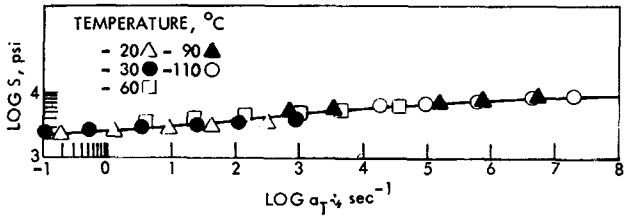


Fig. 24. Shear strength vs. strain rate master curve at −30°C for branched polyethylene.

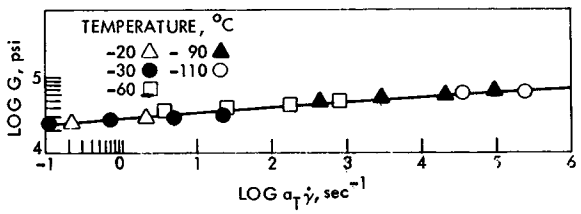


Fig. 25. Shear modulus vs. strain rate master curve at −30°C for branched polyethylene.

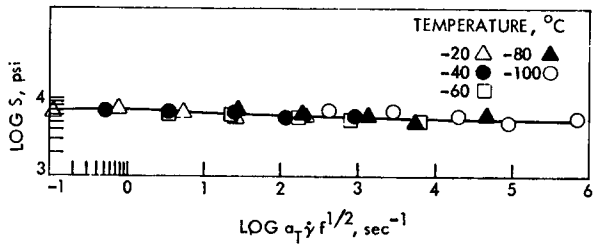


Fig. 26. Shear strength vs. strain rate master curve at −40°C for atactic polypropylene.

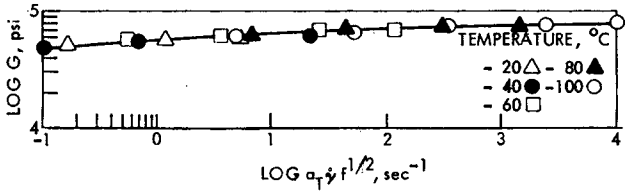


Fig. 27. Shear modulus vs. strain rate master curve at −40°C for atactic polypropylene.

each polymer. In those regimes of temperature and strain rate where success had previously been reported in the use of simple transforms, the simple Arrhenius equation was used to transform the data. In the glassy region or for the highly crystalline polymers, the revised or modified transforms that take into account the vertical shifts as well were used. In essence, the simple transformation procedure is the same as the more complex procedure taking $f$ to be 1. The latter would imply that there are no entanglement couplings or crosslinks in the polymer.

Using as an example the Vistalon 3708, the shear strength data plotted in Figure 6 are replotted on log coordinates. A reference temperature is selected, and every other curve in turn is translated horizontally as well as vertically until it partially overlaps or coincides with the reference curve. The amount of horizontal shift is $a_T$, and that of vertical shift is $f$. The plot of log $(a_T f^{1/2})$ is made against $(1/T - 1/T_0)$, where $T$ is the temperature of the curve being shifted. This is shown in Figure 15. Here, the straight line through the data points is essentially the plot of the Arrhenius equation. For this plot, $T_0$ was taken as 223°K, and the slope of the line gives an activation energy $H_a$ of 10.1 kcal/mol. The data points for var-

TABLE II
Coupling Factor and Activation Energy Values from the Transformation of Shear Properties of Polymers

| Material | Reference temp., °C | Shear strength | | | Shear modulus | | |
|---|---|---|---|---|---|---|---|
| | | $f$ | $H_a$, kcal/mole | Figure number | $f$ | $H_a$, kcal/mole | Figure number |
| Vistalon 3708 | −50 | 1–1.25 | 10.1 | 16 | 1–1.35 | 11.1 | 17 |
| Vistalon 6505 | −70 | 1–1.2 | 9.18 | 18 | 1 | 7.1 | 19 |
| Vistalon 404 | −70 | 1–1.35 | 11.7 | 20 | 1–1.16 | 8.65 | 21 |
| Linear PE | −20 | 1 | 9.33 | 22 | 1 | 10.1 | 23 |
| Branched PE | −30 | 1 | 12.35 | 24 | 1 | 12.25 | 25 |
| Atactic PP | −40 | 1–1.25 | 8.92 | 26 | 1 | 8.3 | 27 |

ious temperatures were then shifted horizontally by log $(a_T f^{1/2})$, as read from the straight line in Figure 15, and vertically by log $(1/f)$. The result is a master curve of shear strength versus strain rate at −50°C, as shown in Figure 16. The same procedure was found to apply successfully to the shear modulus data of Vistalon 3708, giving an activation energy of 11.1 kcal/mole, and the master curve is shown in Figure 17. In the same manner the shear strength and shear modulus data of the other five polymers were transformed, and the master curves are as shown in Figures 18 through 27. Table II shows the reference temperature used for each of the polymers, the activation energy found from the transformation method, and the coupling factor $f$ required to successfully transform the data.

## DISCUSSION

The success of the transformation of shear property data into a master curve by the suggested procedure can be measured by the lack of scatter of data points around the master curve. It is seen from Figures 16 through 27 that there is some scatter, which must be partially due to the inaccuracies in the experimental data and the nonhomogeneity in material. It is significant to note, however, that the reported work compares favorably with other such efforts. From the master curves obtained in this work, it may be seen that 90% of the transformed data points fall within about ±7% error around the master curve. Smith[15] reports an accuracy within about 5% to 7% on the transformation of tensile strength data, using the WLF equation for an amorphous crosslinked GR–S rubber in the rubbery phase, where a vertical transform would not be expected. In the transformations reported by Lohr[6] and Holt[5] for poly(methyl methacrylate) in the glassy state, the scatter is of the order of 25% and 30%, respectively. Those transformations involved mere empirical shifting of the data points, because the shift factors were not controlled by the Arrhenius equation. Furthermore, Holt's transformations were for compressive stresses corresponding to very low strains.

The necessity to use a vertical shift for the successful transformation of shear data of polymers in the glassy state suggests that a morphologic change is taking place in polymers as temperature changes. It can be shown that the shear strength and shear modulus of polypropylene and the Vistalons increase more with a decrease in temperature than predicted by the flexible-chain molecular theory. It must be construed therefore that there are added constraints on the molecule, and these have been called entanglement couplings. The factor $f$ can be taken as a measure of the change in entanglement couplings with temperature. There is at present no way of estimating this change a priori. The use of the factor $f$ in both the horizontal and vertical shifts consistent with the molecular theory of entanglement network provides a theoretical basis for the method. The above successful application of the method to actual data has verified its practical value.

It may be noted that the activation energies quoted in Table II are lower than those usually found in the literature from the transformation of stress relaxation or dynamic mechanical property data. This is due to two factors, namely, the state of the polymer and the type of loading. Bueche[16] and McLoughlin and Tobolsky[17] report that the activation energies in the glassy region are less than in the rubbery region, presumably because of entanglement couplings. Likewise, the loading pattern in the shear tests is likely to cause more severe molecular adjustments and a higher likelihood of entanglement couplings than in the stress relaxation tests. It may therefore be concluded that the activation energy of molecular processes involved in large-strain tensile or shear loading is much smaller than those in stress relaxation or dynamic mechanical loading. As a matter of fact, for metals a considerably lower value of activation energy has been observed for plastic deformation processes than for elastic deformation processes.

The authors appreciate the support of Enjay Polymer Laboratories in supplying the materials and for an Esso research grant for one of us.

## References

1. J. D. Ferry, *Viscoelastic Properties of Polymers*, Wiley, New York, 1961.
2. J. C. Halpin and F. Bueche, *J. Appl. Phys.*, **35**, 3142 (1964).
3. T. L. Smith, *J. Appl. Phys.*, **35**, 27 (1964).
4. H. D. Brettschneider, *Symposium on High Speed Testing*, Interscience, New York, 1960, p. 41.
5. D. L. Holt, *J. Appl. Polym. Sci.*, **12**, 1653 (1968).
6. J. J. Lohr, *Trans. Soc. Rheol.*, **9**, 65 (1965).
7. A. V. Tobolsky, *Properties and Structure of Polymers*, Wiley, New York, 1960.
8. F. Bueche, *J. Appl. Phys.*, **26**, 738 (1955).
9. R. S. Marvin, in *Viscoelasticity—Phenomenological Aspects*, J. T. Bergen, Ed., Academic Press, New York, 1960.
10. E. J. Zapel, *Symposium on Shear and Torsion Testing*, ASTM Special Tech. Publ. No. 289, 1961, p. 26.
11. O. L. Burchett, *Appl. Polym. Symposia*, **No. 5**, 139 (1967).

12. C. C. Hsiao and J. A. Sauer, *J. Appl. Phys.*, **21**, 1071 (1950).
13. P. D. Olear and F. Erdogan, *J. Appl. Polym. Sci.*, **12**, 2563 (1968).
14. R. E. Ely, *Symposium on High Speed Testing*, Interscience, New York, 1960, p. 14.
15. T. L. Smith, *J. Polym. Sci.*, **32**, 99 (1958).
16. F. Bueche, *J. Appl. Phys.*, **28**, 784 (1957).
17. J. McLoughlin and A. Tobolsky, *J. Polym. Sci.*, **8**, 543 (1952).

Received May 11, 1971
Revised October 12, 1971